IEEE Access
Multidisciplinary | Rapid Review | Open Access Journal

Received 4 December 2022, accepted 17 December 2022, date of publication 23 December 2022,
date of current version 29 December 2022.

Digital Object Identifier 10.1109/ACCESS.2022.3232078

RESEARCH ARTICLE

Bit Error Floor Reduction for MQAM Signals in the Presence of Phase Error

YEONSOO JANG, JANGHOON OH, AND HYEONGYONG LIM, (Member, IEEE)
Agency for Defense Development, Daejeon 34186, South Korea

Corresponding author: Hyeongyong Lim (hyeongyonglim@gmail.com)

This work was supported by the Agency for Defense Development by the Korea Government.

ABSTRACT We propose a method to form a non-uniform decision boundary (NUDB) for M-ary quadrature amplitude modulation (MQAM) signals to reduce bit error floor (BEF) in the presence of phase error. We put our focus on angle distances between MQAM symbols and adjacent decision boundaries to observe minimum angle distance, and derive optimum intervals for the decision boundaries to maximize the minimum angle distance. Through computer simulations, we verify that the proposed NUDB shows lower BEF than a conventional uniform decision boundary by 56% and 15% smaller for 16QAM and 64QAM, respectively.

INDEX TERMS Angle distance, bit error floor, non-uniform decision boundary, phase error, quadrature amplitude modulation.

I. INTRODUCTION

Modern high-speed railways require an improved communication system to provide high mobility with high data rate [1]. The latest mobile communication technologies such as 5G and upcoming 6G aim to support superior capabilities with millimeter-wave: Mobility capability of 350 km/h and 500 km/h in 5G and 6G, respectively [2]. However, communication systems for a high-speed platform experience serious Doppler effect in millimeter-wave because Doppler spread increases as both the frequency and the speed of platform increase [3]. Because of large Doppler spread, a phase-locked loop (PLL) requires large loop bandwidth, leading to a decrease of signal-to-noise ratio (SNR) in the loop bandwidth. Due to small SNR in the loop bandwidth, the variance of phase error becomes large, thus the phase error can seriously degrade the bit error rate (BER) performance [4]. On the other side, since a large Doppler spread can cause imperfect channel estimation, a random phase error caused by the imperfect channel estimation also degrades BER performance [5]. Therefore, the phase error is one of the degradation factors in communication systems for high-speed railways [6], [7].

It is very important not only to analyze the BER performance of a communication system for the phase error, but also to improve the performance under noisy phase environments. In the case of constant envelope modulation schemes, the BER performance of binary phase shift keying (BPSK), quadrature phase shift keying (QPSK), and M-ary phase shift keying (MPSK) in the presence of noisy phase reference has been extensively studied in the literature [8], [9], [10], [11], [12]. Especially, bit error floor (BEF) analyses for the random phase error were established in [13] and [14] because a random phase error causes BEF, which is irreducible bit error in a high SNR region. To be specific, Jang et al. [13] proposed a BEF expression of MPSK for Gaussian distributed random phase error and Lee et al. [14] extended BEF analyses for multi-level phase modulation, i.e., amplitude and phase shift keying (APSK). Previous BEF results were mainly focused on a phase modulation such as MPSK. In this paper, we assume that a PLL is used for phase estimation based on a pilot signal and the variance of the phase error is independent of data SNR [13].

M-ary quadrature amplitude modulation (MQAM) signals have been widely used for high-speed data transmission in modern mobile communication systems due to its orthogonality property. BER and BEF analyses for MQAM in the presence of phase noise have been studied in the case of a uniform decision boundary (UBD) [15]. It was observed that the performance of MQAM can be degraded by a random phase error. Because higher-order MQAM signals can be significantly sensitive to the phase error, it is important to reduce

The associate editor coordinating the review of this manuscript and approving it for publication was Dusan Grujić.

the effect of the phase error on communication performance. Recently, Mvone et al. [16] proposed new constellations of 16QAM and 32QAM robust to the phase noise. However, the proposed method in [16] is difficult to compatible with the existing communication system and increases complexity of the receiver because the proposed constellations have a specific configuration, which is not a simple square form.

For high-order MQAM, conventional receiver adopts a uniform decision boundary (UDB) since it is the optimum boundary for an additive white Gaussian noise (AWGN) channel. However, the UDB with the phase error might not be optimal in a high SNR region because the effect of phase error on BEF instead that of AWGN becomes dominant. Indeed, in a high SNR region, BEF is mainly determined by angle distances between symbols and decision boundaries rather than Euclidian distances as pointed out in [14].

The high-order MQAM symbols have various angle distances on a signal constellation, whereas MPSK symbols have uniform angle distances. Moreover, in a high SNR region, the minimum angle distance of MQAM symbols can significantly affect BEF. Thus, BEF of MQAM can be improved by increasing the minimum angle distance.

In this paper, we propose a non-uniform decision boundary (NUDB) for MQAM constellations in order to reduce BEF under random phase errors. We derive angle distances between MQAM symbols and adjacent decision boundaries in the case of arbitrary intervals of decision boundary with the phase error. Then, we derive an optimum interval expression in a closed form for the NUDB to maximize the minimum angle distance. Through computer simulations, we show that the proposed NUDB reduces BEF compared to the UDB.

This paper is organized as follows. Section II describes the system model. In Section III, angle distances of MQAM are analyzed for uniform decision boundary. The optimal interval of non-uniform decision boundaries is derived in Section IV to maximize the minimum angle distance. Section V presents the numerical results. Finally, Section VI concludes the paper.

II. SYSTEM MODEL

When a phase error is present, the k-th received signal of MQAM can be expressed as

$$r_k = x_k e^{-j\theta_k} + n_k, \quad k = 1, 2, \ldots, \tag{1}$$

where x_k is the transmitted MQAM symbol, n_k is the AWGN signal, and θ_k is the phase error.

Real and imaginary components of x_k are selected from the uniform constellation set $\left\{-\left(\sqrt{M}-1\right)d, -\left(\sqrt{M}-3\right)d, \ldots, +\left(\sqrt{M}-3\right)d, +\left(\sqrt{M}-1\right)d\right\}$. The uniform interval $2d$ is the normalized symbol distance given by

$$d = \sqrt{\frac{3\log_2 M E_b}{2(M-1)}}. \tag{2}$$

Note that E_b is the average bit energy.

In communication systems, a PLL can cause the random phase error and the probability density function (PDF) of phase error is assumed to have Gaussian distribution [4], [15]. In (1), θ_k can be modelled as a Gaussian random variable with PDF given as

$$p(\theta_k) = \frac{1}{\sqrt{2\pi}\sigma_\theta}\exp\left(\frac{-\theta_k^2}{2\sigma_\theta^2}\right), \quad -\pi \le \theta \le \pi, \tag{3}$$

where σ_θ is the standard deviation of phase errors [12]. When the normalized loop SNR of PLL is α, the variance of phase error is α^{-1} [13]. Because a high-speed vehicle causes a large Doppler spread, a PLL of the receiver requires a large loop bandwidth to process the frequency spread signal. The large loop bandwidth leads to a decrease in SNR in the loop bandwidth. Due to the small SNR in the loop bandwidth, the variance of phase error becomes large. The phase error with large variance can seriously degrade the BER performance.

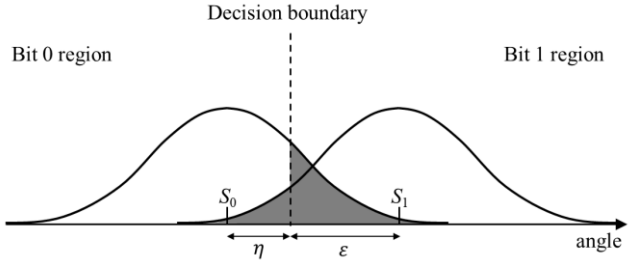

FIGURE 1. Error probability caused by phase error.

In a high SNR region where the effect of AWGN on bit error performance is negligible, the bit error can occur when a transmit symbol rotates and crosses over a decision boundary due to a phase error. We define the angle difference between the transmit symbol and the adjacent decision boundary as the angle distance. Fig. 1 describes the error probability caused by phase error for the two-symbol case. Each symbol has a Gaussian PDF which means the angle of the transmit symbol. The shadowed region depicts the bit error region, and η and ϵ are angle distances for each symbol. To help understanding, a simple two-symbol case is shown as an example, and in the case of MQAM, the decision regions appear more complicated with multiple decision boundaries. However, the most dominant one on error probability is the angular distance between the symbol and the nearest decision boundary. This is analyzed in detail in Section III.

By integrating (3) from angle distances to π as the same approach presented in [14], BEF can be obtained as

$$\begin{aligned} P_{BEF} &= \int_{-\epsilon}^{-\pi} p(\theta)d\theta + \int_{\eta}^{\pi} p(\theta)d\theta \\ &= \int_{\epsilon}^{\pi} p(\theta)d\theta + \int_{\eta}^{\pi} p(\theta)d\theta. \end{aligned} \tag{4}$$

When the value of angle distance is small, it causes large BEF because of the large area of integration in (4). In the following section, we analyze angle distances of MQAM for the UDB.

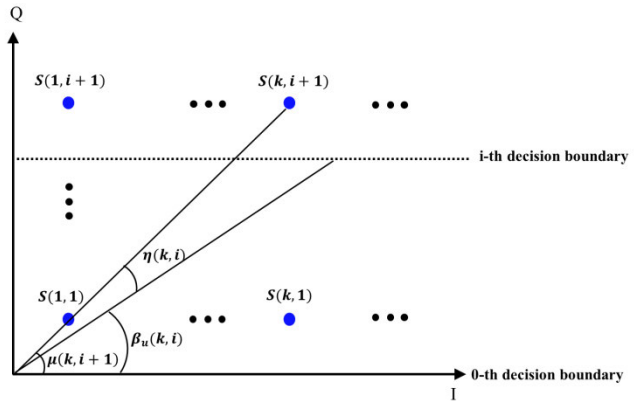

FIGURE 2. Clockwise angle distance of *i*-th decision boundary.

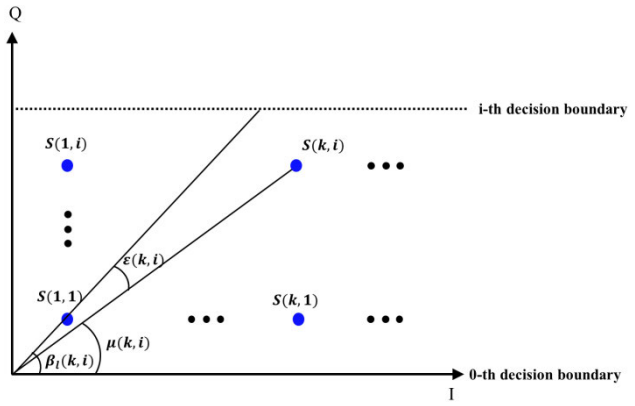

FIGURE 3. Counter-clockwise angle distance of *i*-th decision boundary.

III. ANGLE DISTANCE OF MQAM FOR UNIFORM DECISION BOUNDARY

In a high SNR region, BEF is determined by angle distances between symbols and decision boundaries. Especially, because the angle distances between symbols and adjacent decision boundaries are small, those are dominant on BEF. Thus, we derive and analyze the angle distances between MQAM symbols and adjacent decision boundaries based on the geometry of MQAM constellation. We present results for the quadrature phase by taking advantage of the symmetricity of a MQAM constellation between in-phase and quadrature phase.

First, Fig. 2 shows the clockwise angle distance of the adjacent symbol located above the *i*-th decision boundary for the quadrature phase. By analyzing angle rotations of symbols, the angle distance $\eta\,(k, i)$ between the *i*-th decision boundary and symbols located above the *i*-th decision boundary can be obtained as

$$\begin{aligned}\eta\,(k,i) &= \mu\,(k,i+1) - \beta_u(k,i)\\ &= \tan^{-1}\frac{(2i+1)}{(2k-1)} - \sin^{-1}\frac{2i}{\sqrt{(2k-1)^2+(2i+1)^2}},\end{aligned} \tag{5}$$

TABLE 1. Angle distances for 16QAM.

		$k=1$	$k=2$
$i=1$	$\eta(k,1)$	32.334°	16.875°
	$\epsilon(k,1)$	-	20.797°

TABLE 2. Angle distances for 64QAM.

		$k=1$	$k=2$	$k=3$	$k=4$
$i=1$	$\eta(k,1)$	32.335°	16.875°	10.904°	7.973°
	$\epsilon(k,1)$	-	20.797°	11.784°	8.300°
$i=2$	$\eta(k,2)$	27.019°	15.722°	10.550°	7.828°
	$\epsilon(k,2)$	-	25.529°	12.350°	8.485°
$i=3$	$\eta(k,3)$	23.818°	14.817°	10.237°	7.693°
	$\epsilon(k,3)$	-	-	13.052°	8.688°

where $i = 1, 2, \ldots, \sqrt{M}/2 - 1$ and $k = 1, 2, \ldots, \sqrt{M}/2$. Using (5), the angle distance can be obtained for all the symbols located above the *i*-th decision boundary for MQAM.

Now, Fig. 3 shows the counter-clockwise angle distance of the adjacent symbol located below the *i*-th decision boundary. The angle distance $\epsilon\,(k, i)$ between the *i*-th decision boundary and symbols located below the *i*-th decision boundary can be obtained as

$$\begin{aligned}\epsilon\,(k,i) &= \beta_l\,(k,i) - \mu\,(k,i)\\ &= \sin^{-1}\frac{2i}{\sqrt{(2k-1)^2+(2i-1)^2}} - \tan^{-1}\frac{(2i-1)}{(2k-1)},\end{aligned} \tag{6}$$

where $i = 1, 2, \ldots, \sqrt{M}/2 - 1$ and $k = \mu, \ldots, \sqrt{M}/2$, and μ is the smallest natural number that satisfies $\sqrt{(2\mu-1)^2+(2i-1)^2} > 2i$. It can be easily checked that the angle distance $\epsilon(k, i)$ for k less than μ does not exist because magnitudes of $S\,(1, i), \ldots, S\,(\mu-1, i)$ are less than $2id$ when $\sqrt{(2\mu-1)^2+(2i-1)^2} < 2i$. Using (6), the angle distance for the symbol located below the *i*-th decision boundary can be obtained.

Using (5) and (6), the angle distances of 16 and 64QAM constellations are shown in Table 1 and Table 2. We can see that $\epsilon\,(k, i) > \eta\,(k, i)$ for the same i. For the *i*-th decision boundary, the angle distance $\eta\left(\sqrt{M}/2, i\right)$ for the outermost symbol $S(\sqrt{M}/2, i+1)$, is the minimum angle distance, that is, the angle distance $\eta\left(\sqrt{M}/2, i\right)$ is the most dominant factor for determining BEF. If the decision boundary is set to maximize the minimum angle distance, BEF can be reduced.

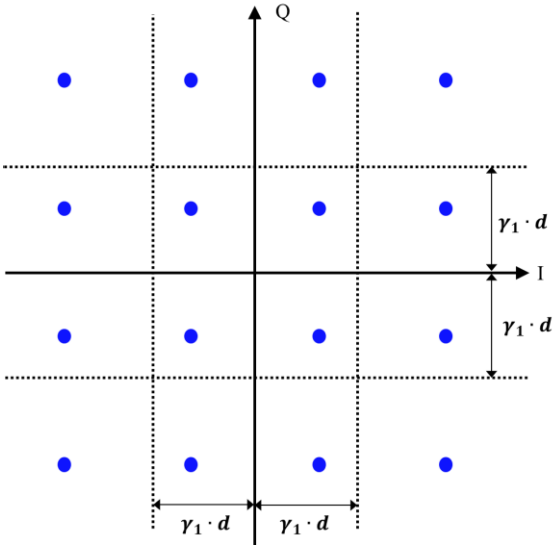

FIGURE 4. 16QAM constellation with NUDB.

Therefore, in the following section, we propose a NUDB that can maximize the minimum angle distance and derive the optimal decision boundary intervals.

IV. NON-UNIFORM DECISION BOUNDARY FOR MQAM

As shown in Fig. 1, maximizing the minimum angle distance is identical to maximizing the conditional probability density for the correct bit. The minimum angle distance is determined by the interval between the symbol and the adjacent decision boundary. Therefore, the error probability caused by phase error can be minimized by deriving the decision boundary interval to maximize the minimum angle distance. In order to reduce BEF by increasing the minimum angle distance, we propose a NUDB for MQAM, which is not a UDB with the conventional $2d$ interval.

Fig. 4 depicts an example of a 16QAM constellation with the NUDB. The distance from the axis to the i-th decision boundary for the NUDB is set as $\gamma_i d$, while the distance for the UDB is $2di$. Note that γ_i is the interval coefficient of the i-th decision boundary. As discussed in the previous section, the minimum angle distance of each decision boundary is defined as $\eta\left(\sqrt{M}/2, i\right)$. It can be easily checked that γ_i becomes smaller than $2i$ to increase $\eta\left(\sqrt{M}/2, i\right)$. On the contrary, when γ_i becomes smaller, $\epsilon\left(\sqrt{M}/2, i\right)$ decreases.

Therefore, the minimum angle distance can be maximized by obtaining γ_i that satisfies the boundary condition $\epsilon\left(\sqrt{M}/2, i\right) = \eta\left(\sqrt{M}/2, i\right)$ due to the fact that the MQAM symbols are transmitted equally likely and the likelihood functions are symmetric. This condition can be written as

$$\sin^{-1}\left(\frac{\gamma_i}{L_i}\right) + \sin^{-1}\left(\frac{\gamma_i}{H_i}\right) = \tan^{-1}\left(\frac{2i+1}{\sqrt{M}-1}\right) + \tan^{-1}\left(\frac{2i-1}{\sqrt{M}-1}\right), \quad (7)$$

TABLE 3. Optimum interval coefficients for 16 and 64QAM.

	$M = 16$	$M = 64$
γ_1	1.8974	1.9799
γ_2	-	3.9598
γ_3	-	5.9397

where $L_i = \sqrt{\left(\sqrt{M}-1\right)^2 + (2i-1)^2}$ and $H_i = \sqrt{\left(\sqrt{M}-1\right)^2 + (2i+1)^2}$. Using sum formula for arcsine ($\sin^{-1}x + \sin^{-1}y = \sin^{-1}\left(x\sqrt{1-y^2} + y\sqrt{1-x^2}\right)$), (7) can be rewritten as

$$\sin^{-1}\left(\frac{\gamma_i}{L_i}\sqrt{1-\frac{\gamma_i^2}{H_i^2}} + \frac{\gamma_i}{H_i}\sqrt{1-\frac{\gamma_i^2}{L_i^2}}\right) = \tan^{-1}\left(\frac{2i+1}{\sqrt{M}-1}\right) + \tan^{-1}\left(\frac{2i-1}{\sqrt{M}-1}\right). \quad (8)$$

From (8), we can obtain the equation for γ_i as

$$\gamma_i^2\left\{\frac{1}{L_i^2} + \frac{1}{H_i^2} - \frac{2\gamma_i^2}{L_i^2 H_i^2} + \frac{2}{L_i^2 H_i^2}\sqrt{\left(L_i^2-\gamma_i^2\right)\left(H_i^2-\gamma_i^2\right)}\right\} = T_i^2, \quad (9)$$

where $T_i = \sin\left(\tan^{-1}\left(\frac{2i+1}{\sqrt{M}-1}\right) + \tan^{-1}\left(\frac{2i-1}{\sqrt{M}-1}\right)\right)$.

Let $\beta_i = \gamma_i^2$, (9) can be expressed in terms of β_i as

$$\left\{\frac{\left(L_i^2-H_i^2\right)^2}{4} + L_i^2 H_i^2 T_i^2 - L_i^2 H_i^2\right\}\beta_i^2 - \frac{\left(L_i^2-H_i^2\right)L_i^2 H_i^2 T_i^2}{2}\beta_i + \frac{L_i^4 H_i^4 T_i^4}{4} = 0. \quad (10)$$

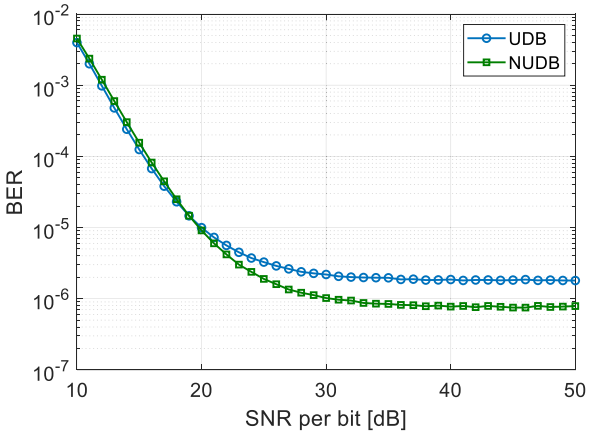

FIGURE 5. BEF of 16QAM for AWGN channel.

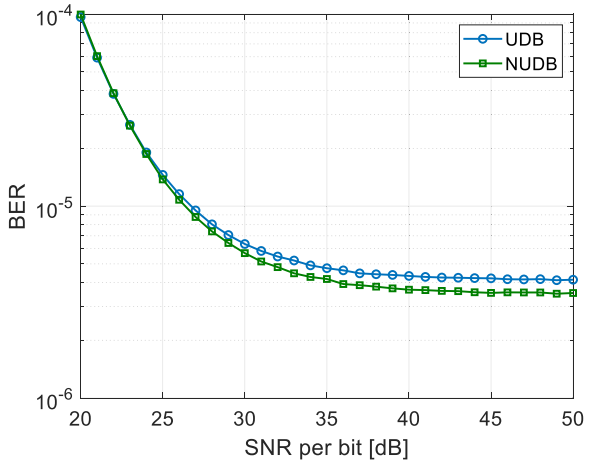

FIGURE 6. BEF of 64QAM for AWGN channel.

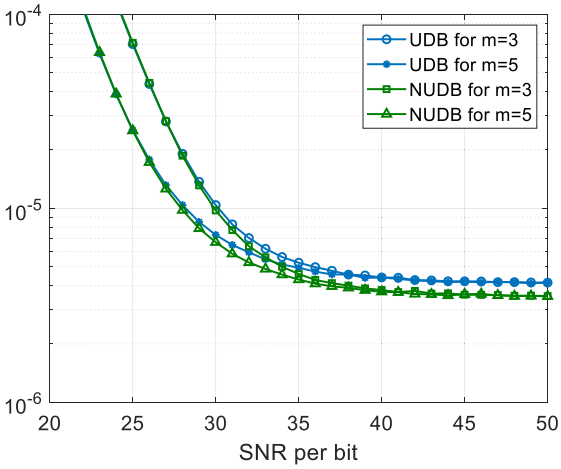

FIGURE 8. BEF of 64QAM for fading channel.

Solving the quadratic equation (10), we finally obtain the solution of γ_i as

$$\gamma_i = \sqrt{\frac{\left(L_i^2 + H_i^2\right) - 2L_iH_i\sqrt{1 - T_i^2}}{\frac{\left(L_i^2 - H_i^2\right)^2}{L_i^2H_i^2T_i^2} + 4}}. \tag{11}$$

Finally, using (11), the optimum interval of the i-th decision boundary that minimizes BEF can be straightforwardly obtained for MQAM signals. As examples, Table 3 shows γ_i for 16 and 64QAM.

Note that the interval coefficient γ_i is $2i$ in the case of UDB. When the NUDB is adapted with the suggested interval coefficient obtained by (11), BEF can be reduced by increasing the minimum angle distance. It is noteworthy that the NUDB can be easily implemented by applying the optimum interval coefficients for the MQAM signal decision in the existing receiver structure.

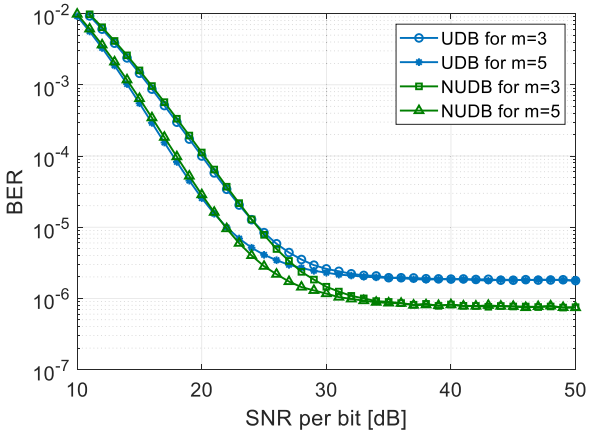

FIGURE 7. BEF of 16QAM for fading channel.

Because the proposed NUDB can reduce BEF without complexity increase of hardware and software, it can be very practical and useful for communication systems in the presence of phase error.

V. NUMERICAL RESULTS

In this section, we present BEF performance under the effect of phase error using Monte-Carlo simulations. Then, we verify that BEF performance can be improved for the proposed NUDB. As for the conditions of simulation, 1,000,000 MQAM symbols were generated with equal probability for each SNR and the number of error bit was counted for the UDB and NUDB. In Figs. 5 and 6, we plot BEF of 16QAM and 64QAM for the UDB and NUDB in AWGN channel when the deviations of the phase error are 4° and 2° for 16QAM and 64QAM, respectively [15]. In addition, Figs. 7 and 8 depict BEF of 16QAM and 64QAM for the UDB and NUDB in Nakagami-m fading channel.

As shown in the figures, BER performance in the fading channel is worse than that in the AWGN channel but BEF in fading channel converges to the same value as BEF in the AWGN channel. This phenomenon is verified for MPSK in [13] and we confirmed that for MQAM in this paper.

We can see that BER of the UDB is slightly less in a low SNR region. However, in a high SNR region, BEF is reduced when the NUDB is applied. For 16QAM, BEF of the UDB is 1.798×10^{-6}, and BEF of the NUDB is 7.875×10^{-7}, which is about 56% smaller than that of the UDB. For 64QAM, BEF of the UDB is 4.134×10^{-6} and BEF of the NUDB is 3.525×10^{-6}, which is about 15% smaller than that of the UDB. Through these results, we can observe that the application of NUDB to the receiver can improve BEF under a random phase error.

When the constellation of 16QAM proposed in [16] is adopted, low BEF can be achieved which is lower than that of the proposed method of 16QAM in the same simulation environment. However, to obtain optimal performance for the specific constellation, M complex multiplications and comparisons per one symbol decision are required in the receiver because Euclidian distances between the received symbol

and all candidate symbols should be calculated, whereas the proposed method requires only a few comparisons because the conventional constellation of a simple square form is used. Thus, the proposed method is more practical with very low complexity and has compatibility with the existing communication system.

From the Figs. 5 and 6, we can also see that the better BEF reduction performance is achieved for low-order QAM signals. Because of the large distance between the signal points of low-order QAM, the differences between angle distances are larger than high-order QAM as shown on Tables 1 and 2. As a result, there is the opportunity for improving the minimum angle distance for the low-order QAM constellation.

VI. CONCLUSION

In this paper, we proposed the NUDB to reduce BEF of MQAM in a noisy phase situation. Through the derived angle distance expressions for the MQAM symbols and adjacent decision boundaries, it was confirmed that the outermost symbol located above each decision boundary has the minimum angle distance, and the outermost symbol located below has the second minimum angle distance. The optimum interval for the NUDB that maximizes the minimum angle distance was derived, and it was verified that BEF of the NUDB is improved compared to that of the UDB through computer simulations. The proposed NUDB is highly practicable because it can reduce BEF only by setting the value of the decision boundary without implementing additional hardware and software when there is a random phase error. In this paper, we focused on phase error which is one of the impairments in communication systems. As future work, an improved method can be expected for various impairments, such as I/Q imbalance and nonlinearity of a high-power amplifier.

REFERENCES

[1] R. He, B. Ai, G. Wang, K. Guan, Z. Zhong, A. F. Molisch, C. Briso-Rodriguez, and C. P. Oestges, "High-speed railway communications: From GSM-R to LTE-R," *IEEE Veh. Technol. Mag.*, vol. 11, no. 3, pp. 49–58, Sep. 2016.

[2] S. Henry, A. Alsohaily, and E. S. Sousa, "5G is real: Evaluating the compliance of the 3GPP 5G new radio system with the ITU IMT-2020 requirements," *IEEE Access*, vol. 8, pp. 42828–42840, 2020.

[3] T. Levanen, J. Talvitie, R. Wichman, V. Syrjala, M. Renfors, and M. Valkama, "Location-aware 5G communications and Doppler compensation for high-speed train networks," in *Proc. EuCNC*, Oulu, Finland, Jun. 2017, pp. 1–6.

[4] A. J. Viterbi, "Phase-locked loop dynamics in the presence of noise by Fokker-Planck techniques," *Proc. IEEE*, vol. 51, no. 12, pp. 1737–1753, Dec. 1963.

[5] X. Tang, M.-S. Alouini, and A. J. Goldsmith, "Effect of channel estimation error on M-QAM BER performance in Rayleigh fading," *IEEE Trans. Commun.*, vol. 47, no. 12, pp. 1856–1864, Dec. 1999.

[6] J. Talvitie, T. Levanen, M. Koivisto, T. Ihalainen, K. Pajukoski, and M. Valkama, "Positioning and location-aware communications for modern railways with 5G new radio," *IEEE Commun. Mag.*, vol. 57, no. 9, pp. 24–30, Sep. 2019.

[7] K. Xu, Z. Shen, Y. Wang, and X. Xia, "Location-aided mMIMO channel tracking and hybrid beamforming for high-speed railway communications: An angle-domain approach," *IEEE Syst. J.*, vol. 14, no. 1, pp. 93–104, Mar. 2020.

[8] V. K. Prabhu, "PSK performance with imperfect carrier phase recovery," *IEEE Trans. Aerosp. Electron. Syst.*, vol. AES-12, no. 2, pp. 275–286, Mar. 1976.

[9] G. Kaplan and U. Ram, "Bounds on performance for the noisy reference PSK channel," *IEEE Trans. Commun.*, vol. 38, no. 10, pp. 1699–1707, Oct. 1990.

[10] P. Y. Kam, S. K. Teo, Y. K. Some, and T. T. Tjhung, "Approximate results for the bit error probability of binary phase shift keying with noisy phase reference," *IEEE Trans. Commun.*, vol. 41, no. 7, pp. 1020–1022, Jul. 1993.

[11] Y. Some and P. Kam, "Bit-error probability of QPSK with noisy phase reference," *IEE Proc., Commun.*, vol. 142, pp. 292–296, Oct. 1995.

[12] Y. Jang, D. Yoon, and S.-K. Lee, "Generalized BER expression of MPSK in the presence of phase error," *IEEE Commun. Lett.*, vol. 17, no. 12, pp. 2213–2216, Dec. 2013.

[13] Y. Jang, J. Jeong, and D. Yoon, "Bit error floor of MPSK in the presence of phase error," *IEEE Trans. Veh. Technol.*, vol. 65, no. 5, pp. 3782–3786, May 2016.

[14] J. Lee, Y. Jang, and D. Yoon, "Bit error floor of multi-level phase modulation with noisy phase reference," *IET Electron. Lett.*, vol. 53, no. 13, pp. 862–864, Jun. 2017.

[15] H. Jafari, H. Miar-Naimi, and J. Kazemitabar, "Bit error probability of MQAM in the presence of phase noise," *IEEE Trans. Veh. Technol.*, vol. 69, no. 12, pp. 14918–14931, Dec. 2020.

[16] R. E. Mvone, C. Hannachi, D. Hammou, E. Moldovan, and S. O. Tatu, "Optimization of 16-QAM and 32-QAM constellations for mitigating impairments of phase noise in millimeter-wave receivers," *IEEE Trans. Wireless Commun.*, vol. 21, no. 6, pp. 3605–3616, Jun. 2022.

YEONSOO JANG received the B.S. and Ph.D. degrees in electronic communications engineering from Hanyang University, Seoul, South Korea, in 2009 and 2015, respectively. Since 2015, he has been with the Agency for Defense Development, Daejeon, South Korea. His research interests include communication theory, wireless communication systems, wideband signal processing, and electronic warfare.

JANGHOON OH received the B.S. degree in electronic communication engineering from Hanyang University, Seoul, South Korea, in 1996, the M.S. degree in electrical and computer engineering from the University of California at Irvine, Irvine, CA, USA, in 2006, and the Ph.D. degree in electronics and computer engineering from Hanyang University, in 2018. From 1996 to 2004, he was a Technical Manager at the Network Strategy Division, SK Telecom, South Korea. From 2009 to 2011, he was a Senior Manager at the Corporate Planning Division, NCsoft, South Korea. From 2018 to 2019, he was an Assistant Professor with Kyungmin University, Uijeongbu-si, South Korea. Since 2019, he has been a Principal Researcher with the Agency for Defense Development, Daejeon, South Korea. His research interests include wireless communication networks and military tactical communications.

HYEONGYONG LIM (Member, IEEE) received the B.S. and Ph.D. degrees in electronics and computer engineering from Hanyang University, Seoul, South Korea, in 2012 and 2018, respectively. Since 2018, he has been a Senior Researcher with the Third Research and Development Institute and the Defense Test and Evaluation Research Institute, Agency for Defense Development, Daejeon, South Korea. His research interests include statistical signal processing with applications in detection and estimation theory, information theory, and communication theory.